

Estimating numerical errors due to operator splitting in global atmospheric chemistry models: transport and chemistry.

Mauricio Santillana^{a,*}, Lin Zhang^b, Robert Yantosca^a

^a*School of Engineering and Applied Sciences, Harvard University, Cambridge, MA 02138, United States*

^b*Laboratory for Climate and Ocean-Atmosphere Sciences, Department of Atmospheric and Oceanic Sciences, School of Physics, Peking University, Beijing, 100871, China*

Abstract

We present upper bounds for the numerical errors introduced when using operator splitting methods to integrate transport and non-linear chemistry processes in global chemical transport models (CTM). We show that (a) operator splitting strategies that evaluate the stiff non-linear chemistry operator at the end of the time step are more accurate, and (b) the results of numerical simulations that use different operator splitting strategies differ by at most 10%, in a prototype one-dimensional non-linear chemistry-transport model. We find similar upper bounds in operator splitting numerical errors in global CTM simulations.

Keywords: Atmospheric chemistry, operator splitting, model verification, numerical errors

1. Introduction

Global tropospheric chemistry transport models (CTM) are used to address important issues ranging from air quality to climate change. In order to continuously improve their performance, it is of crucial importance to understand and quantify the diverse sources of uncertainties and errors present in them. We group these in three different categories, (i) errors and uncertainties coming from observations and data used in our models (such as emission inventories, wind fields, reaction rates); (ii) errors coming from our choice of governing equations (or mathematical model), parametrizations, and the level of complexity of the physical modules included in our formulation; and (iii) numerical errors coming from the choice of algorithms we use to solve the governing equations using computers (Enting, 2002; Zhang et al, 2011).

In this study, we focus our attention on estimating the magnitude of numerical errors (iii), in particular, those arising from the choice of operator splitting technique utilized to integrate in time the transport and chemistry

operators in global CTMs. In order to achieve this, we numerically extend the results introduced for the linear diffusion-reaction case in (Sportisse, 2000), to a non-linear 1-D chemistry-transport numerical model. The latter numerical results provide us with a framework to estimate upper bounds for operator splitting errors in the fully non-linear 3-D state-of-the-art global CTM: GEOS-Chem (Bey et al., 2001).

Global CTMs simulate the dynamics of chemical species in the atmosphere by numerically integrating a set of coupled nonlinear partial differential equations of the type:

$$\frac{\partial C_i}{\partial t} + \mathbf{u} \cdot \nabla C_i = P_i - L_i, \quad i = 1, \dots, N \quad (1)$$

where $C_i(\mathbf{x}, t)$ represents the spatio-temporal evolution of the concentration of species i (typically over a hundred species are considered), $\mathbf{u}(\mathbf{x}, t)$ is the wind velocity, and $P_i = P_i(\{C_j\}, \mathbf{x}, t)$ and $L_i = L_i(\{C_j\}, \mathbf{x}, t)$ are the ensemble of atmospheric sources and sinks, respectively.

The chemistry operator on the right-hand-side of equations (1) models the chemical interaction of atmospheric species whose lifetimes range from milliseconds to many years. The chemistry operator is very stiff as a consequence of this large range of time-scales

*Corresponding author. Tel.: 617 495-2891

Email addresses: msantill@fas.harvard.edu (Mauricio Santillana), zhanglg@pku.edu.cn (Lin Zhang), yantosca@seas.harvard.edu (Robert Yantosca)

and thus, implicit-in-time methods are an appropriate choice to integrate equations (1). Traditional methods, such as the method of lines, aimed at achieving this task in realistic 3D simulations, involve solving for an enormous number of degrees of freedom at each time step in a coupled fashion ($10^8 \approx 100$ chemical species in $\sim 10^6$ grid cells, for a $1^\circ \times 1^\circ$ spatial resolution). This is due to the inter-species coupling in the chemistry operator and the spatial coupling in the transport operator. In practical situations, however, efficient computational algorithms to integrate equations (1) use operator splitting strategies that allow the explicit time-integration of the transport and implicit time-integration of the chemistry operators separately and sequentially, thus, reducing significantly the degrees of freedom solved in a coupled fashion at a given time step. This is done at the expense of a loss of accuracy in the approximate solution (Hundsdorfer and Verwer, 2003).

The magnitude of the numerical errors introduced by the time-integration of equations (1) in realistic 3-D computer simulations is a hard task since no relevant analytic solution can be used as a reference to estimate them. In theory, estimates of these errors depend directly on the regularity properties of the analytic solution of equations (1), the set of initial and boundary conditions, and the chosen numerical scheme (Iserles, 2009; Ern and Guermond, 2004; Brenner and Scott, 2008). In this study, we assume that the analytic solution of equations (1) is unique and regular enough so that numerical error estimates can be expressed as inequalities of the form (2). Operator splitting errors, as well as numerical errors arising from the time-integration of the chemistry operator depend explicitly on the magnitude of the chosen time steps, while numerical errors coming from the time-integration of the transport operator depend both on the time step and on the grid size. This fact, in combination with an expression of the analytic solution of equations (1), is exploited to obtain the exact magnitude of operator splitting errors in our one-dimensional proto-type transport-chemistry numerical model.

Our one-dimensional numerical experiments show three main results: (a) operator splitting sequences where the stiff non-linear chemistry operator is evaluated at the end of the time step are more accurate than those where the transport is evaluated lastly, independently of the operator splitting time-step, as in the linear case introduced in (Sportisse, 2000); (b) the results of numerical simulations that use different operator splitting strategies differ by at most 10%; and (c) numer-

ical errors coming from the integration of the transport operator are much bigger than those coming from the operator splitting technique for spatial and temporal scales comparable to those used in global CTM. We use this fact, and evidence from papers such as (Wild and Prather, 2006; Rastigeyev et al., 2007; Prather et al., 2008; Santillana, 2013), to suggest that in realistic 3D simulations, errors due to operator splitting are much smaller than those introduced by transport schemes.

2. Numerical error estimation

Upper bounds of the numerical errors introduced by solving partial differential equations with regular boundary and initial conditions, using a given numerical scheme, can be expressed by inequalities represented as

$$\|C(x, t) - C_h(x, t)\|_{V_1} \leq M_1 \Delta t^\alpha + M_2 \Delta x^\beta \quad (2)$$

where $C(x, t)$ is the true solution of the partial differential equation, $C_h(x, t)$ the numerical approximation, Δt and Δx are the time step and grid size respectively, α and β are exponents (typically larger than one) that determine the order of convergence of the method in time and space respectively, M_1 and M_2 are constants that depend on the regularity of the true solution $C(x, t)$ and parameters in the equation, and $\|\cdot\|_{V_1}$ is the norm in the appropriate Banach space V_1 . For a convergent method, as $\Delta t \rightarrow 0$ and $\Delta x \rightarrow 0$, the numerical error vanishes, (*i.e.* $\|C - C_h\|_{V_1} \rightarrow 0$) and the numerical approximation C_h converges to the true solution C , in the normed space V_1 (Iserles, 1996; Ern and Guermond, 2004; Brenner and Scott, 2002).

For the specific set of partial differential equations (1), operator splitting errors and errors coming from the numerical integration of the chemistry operator (where no coupling in space exists) contribute to the first term on the right-hand-side of inequality (2), whereas, numerical errors from the integration of the transport operator contribute to the first and second terms of the right-hand-side of inequality (2). Quantifying the independent contribution of each processes to each term of inequality (2) is not simple in practical applications. In the following section, we show how to estimate the magnitude of operator splitting errors in the absence of other numerical error coming from the time-integration of the transport and chemistry operators.

2.1. Operator splitting techniques and error estimation

Classical approaches to estimate the numerical errors introduced by operator splitting approaches are based

on asymptotic expansions of exponential operators (linear case) and Lie operator formalism (nonlinear case). For completeness, we briefly describe important results of the linear analysis of operator splitting methods in this section. We refer the reader to Lansen and Verwer (1999); Sportisse (2000); Hundsdorfer and Verwer (2003) and the references therein for more details. In this section, it is assumed that the time-integration of each operator separately can be found exactly giving rise to no numerical error, *i.e.* the numerical errors discussed below come only from the choice of the operator splitting technique.

We use as an example the linear evolution equation,

$$\frac{dv}{dt} = Av + Bv, \quad v(0) = v_0, \quad v \in \mathbb{R}^n \quad (3)$$

where A and B are linear operators. One of these operators could represent the linear spatial differential operator d/dx (transport) in equations (1). The analytic solution for this problem is given by:

$$v = v_0 \exp((A + B)t) \quad (4)$$

The simplest operator splitting method, called Godunov and denoted by $(A - B)$, can be obtained for $t \in [0, \Delta t]$ by solving the two evolution equations in sequence as:

$$\begin{cases} \frac{dv^*}{dt} = Av^*, & v^*(0) = v_0 & \text{in } [0, \Delta t] \\ \frac{dv^{**}}{dt} = Bv^{**}, & v^{**}(0) = v^*(\Delta t) & \text{in } [0, \Delta t]. \end{cases} \quad (5)$$

The value for v at $t = \Delta t$ is given by $v_{AB}(\Delta t) = v^{**}(\Delta t)$. The solution obtained with this operator splitting method at $t = \Delta t$ is given by

$$v_{AB}(\Delta t) = v_0 \exp(B\Delta t) \exp(A\Delta t) \quad (6)$$

The exact solution (4) and the solution v_{AB} in the previous equation will be the same if

$$\exp((A + B)\Delta t) = \exp(B\Delta t) \exp(A\Delta t).$$

This will happen if the operators A and B commute (think of matrices), *i.e.* if $AB = BA$. When $AB \neq BA$, then the (point-wise) local-in-time numerical error associated to solving problem (3) using Godunov's operator splitting technique can be shown to be

$$le_{AB} = \frac{(AB - BA)}{2} \Delta t^2 v_0 \quad (7)$$

which leads to a global error $O(\Delta t)$, *i.e.* $\|v - v_{AB}\| \leq M_{AB} \Delta t$ (for a constant M_{AB} that depends only on the regularity of the analytic solution

v). Since the numerical error vanishes as $\Delta t \rightarrow 0$, Godunov's method is a convergent first order method in time, in the linear case. Another simple Godunov operator splitting can be obtained by reversing the order of evaluation of the operators A and B to obtain the $(B - A)$ method (v_{BA}). A more accurate and symmetric operator splitting method, often referred to as Strang method (Strang, 1968), can be obtained by averaging the output of the two previous methods, *i.e.* $v_S(\Delta t) = \frac{1}{2}(v_{AB} + v_{BA})$. It can be shown that the Strang operator method is globally second order accurate, *i.e.* $\|v - v_S\| \leq M_S \Delta t^2$ for a constant M_S (Sportisse, 2000; Hundsdorfer and Verwer, 2003).

The linear analysis presented above may fail and lead to different convergence results if one of the operators is stiff, *i.e.* if the dynamics of one operator take place in much faster time scales than the dynamics in the other operator (Sportisse, 2000). This can be seen by introducing a small parameter ϵ (representing the ratio between fast time scales in the stiff operator and the slow time scales of the other operator) and re-writing the linear evolution equation (3) as a singular perturbation equation by re-defining

$$A = \frac{\chi(\epsilon)}{\epsilon} \quad \text{and} \quad B = T. \quad (8)$$

For our purposes, one can identify the chemistry operator with the stiff operator χ/ϵ , (the nonlinear chemistry can be, locally-in-time and space, approximated by a linear and stiff mechanism at least for some subset of fast species), and identify the transport operator with the slow operator T , for which the dynamics takes place in a more confined range of time scales (as represented by our global models). It is shown in (Sportisse, 2000) that the local error for the $(\frac{\chi}{\epsilon} - T)$ Godunov method becomes (compare to equation (7)):

$$le_\epsilon \sim \frac{(\chi T - T \chi)}{\epsilon} \Delta t^2 v_0 \quad (9)$$

leading to a global error $O(\frac{\Delta t}{\epsilon})$, implying that $\|v - v_\epsilon\| \leq M_\epsilon (\frac{\Delta t}{\epsilon})$. Note that convergence of the operator splitting method, in this case, can only be guaranteed provided the operator splitting time step, Δt , is small enough to satisfy $\Delta t \ll \epsilon$ so that higher order terms, $O(\frac{\Delta t}{\epsilon})^k$, will indeed vanish as $k \rightarrow \infty$ in the Taylor expansion of the error.

In atmospheric chemistry simulations, we use operator splitting methods to integrate in-time two operators in equations (1): transport and chemistry. Trans-

port and chemistry are known to commute when the velocity field is divergent free and chemistry is independent of the spatial location. In real atmospheric situations, these conditions are typically not met. Indeed, the non-linear chemistry operator depends dynamically on the geographic location (due to photolysis), and atmospheric wind fields are in general not divergent-free.

The result of the linear analysis above suggests that operator splitting approaches will converge only if the operator splitting time step is much smaller than the lifetime of the fastest species in the chemistry mechanism ($\Delta t \ll \epsilon$). This is also the criterion established to ensure stability and convergence of explicit-in-time chemistry solvers, and suggests the use of prohibitively small operator splitting time-steps in order to guarantee convergence of the method. In practice, however, the use of implicit schemes to integrate the chemistry operator in global chemistry models leads to the choice of large operator splitting time-steps compared to the intrinsic stiffness of the chemistry system ($\Delta t \gg \epsilon$). As a consequence, and according to expression (9), we may expect to observe large operator splitting errors when solving equations (1) with stiff and potentially non-linear chemistry operators.

It is argued in Sportisse (2000), that operator splitting errors, even in the presence of large operator splitting time steps (such that $\Delta t \gg \epsilon$), may not be as big as suggested by expression (9). Sportisse (2000) argues that the stiffness of the system can be balanced by the existence of an underlying reduced model (low-dimensional manifold) describing the dynamics of the system and thus, by choosing the appropriate order of operator evaluation in a time-step, the splitting error may be bounded even with the increase of stiffness. Moreover, he shows for the linear case that sequences where the stiff operator is evaluated at the end of the time step lead to convergent and accurate methods in a one dimensional diffusion-chemistry toy example, even for large operator splitting time steps. In solving equations (1), examples of these sequences include: Transport-Chemistry and Chemistry-Transport-Chemistry.

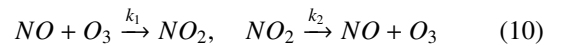
Intuitively speaking, evaluating the transport operator at the end of the time step sets the state the system far from the underlying low dimensional manifold driving the chemical system and provides an initial condition v_0 for the next time evaluation that enhances error propagation. This is avoided by evaluating the stiff chemistry operator at the end of the time step. The existence of these reduced models driving the dynamics in regional and global atmospheric chemistry models

has been found in Lowe and Tomlin (2000); Santillana et al. (2010); Rastigeyev et al. (2007), suggesting that the operator splitting order should be selected carefully. To the best of our knowledge, a careful investigation of these errors in the realistic non-linear case does not exist so far and thus we aim at achieving this here.

Isolating operator splitting errors in practical global atmospheric chemistry models is not straightforward, first, because we lack expressions for the analytic solution of the system in realistic circumstances, and second, since the solutions of the chemistry and transport operators, separately, are obtained using numerical schemes and thus are not exact as it was assumed in the previous analysis. In order to estimate upper bound estimates of operator splitting errors we proceeded as follows. We first find sharp estimates of numerical errors in a 1D non-linear chemistry-transport prototype problem with a known analytic solution. We designed this 1D problem to resemble the interaction of numerical errors in the time-integration of the transport and (stiff) non-linear chemistry, when using operator splitting methods, at spatial and time scales utilized in 3D global simulations. Our 1D findings guide our methodology to understand the differences observed between the outputs of 3D global simulations using different operator splitting strategies.

3. One-dimensional advection-reaction system

We considered a one-dimensional advection-reaction system that can be solved analytically and thus exact values of numerical errors can be obtained. The system is characterized by a constant wind field throughout the domain, and a three-species (NO , NO_2 , O_3) stiff non-linear chemistry-mechanism modeling the $NO_x(NO + NO_2)$ cycle through oxidation by ozone (O_3). This cycle is key in determining the balance of Ozone (O_3) in the atmosphere. The chemical reactions are given by:



where the parameters k_1 and k_2 represent the constant reaction rates throughout the domain. The resulting advection-reaction system of equations can be written as

$$\frac{\partial NO}{\partial t} + u \frac{\partial NO}{\partial x} = -k_1(NO) O_3 + k_2 NO_2 \quad (11)$$

$$\frac{\partial NO_2}{\partial t} + u \frac{\partial NO_2}{\partial x} = k_1(NO) O_3 - k_2 NO_2 \quad (12)$$

$$\frac{\partial O_3}{\partial t} + u \frac{\partial O_3}{\partial x} = -k_1(NO) O_3 + k_2 NO_2 \quad (13)$$

where NO , NO_2 , and O_3 , represent the concentration of each chemical in space and time, and u the constant velocity of the flow (compare with equations (1)).

The advection and reaction operators commute in this problem (since the advection operator is divergent-free, $\partial u/\partial x = 0$, and the chemistry is independent of the location in space), thus, the use of operator splitting approaches should not introduce any error when the exact solutions of the chemistry and advection operators are known. However, when solving numerically the advection operator, with an Eulerian advection scheme, undesired numerical diffusion will cause the numerical advection operator to not commute with the chemistry operator (since nonlinear chemical operators do not commute with diffusion, as shown in Hundsdorfer and Verwer (2003)) thus signalling the emergence of operator splitting errors in the numerical solution of equations (11)-(13).

This one-dimensional problem is relevant in realistic global 3D simulations since the transport operator is solved utilizing Eulerian numerical schemes, and thus, giving rise to undesired numerical diffusion that will not commute with the time-integration of the chemistry operator. Moreover, in regions in the atmosphere where the flow is near (2D) divergent-free (due to a well stratified atmosphere) and during the night (or day) so that chemistry is independent of space, chemistry and transport operators may commute locally in space and time as in the 1D prototype.

In more complicated circumstances, for example in regions of space close to the terminator line (where the day and night boundary is), and in Equatorial regions where convection makes the atmosphere be far from divergent-free conditions, operator splitting errors can be expected to be larger since the advection and chemistry operators will not commute.

3.1. Analytic steady-state solution

When the chemistry is fast with respect to transport processes, an exact expression can be found for the steady-state solution of system (11)-(13). For example, by choosing $k_1 = 1000$ and $k_2 = 2000$, as in (Sportisse, 2000), and introducing the non-stiff combined-chemistry operator $\chi = (NO) O_3 - 2 NO_2$, we can represent a stiff (fast) chemistry operator as the quotient χ/ϵ for a small parameter ϵ . Equations (11-13)

can be re-written, as suggested in equation (8), as:

$$\frac{\partial NO}{\partial t} + u \frac{\partial NO}{\partial x} = -\frac{\chi}{\epsilon}, \quad (14)$$

$$\frac{\partial NO_2}{\partial t} + u \frac{\partial NO_2}{\partial x} = \frac{\chi}{\epsilon}, \quad (15)$$

$$\frac{\partial O_3}{\partial t} + u \frac{\partial O_3}{\partial x} = -\frac{\chi}{\epsilon}. \quad (16)$$

Here ϵ represents the stiffness of the system and is given by the ratio between the slow advection scales and the fast chemistry time scales. For example if $u \sim O(1)$ and $k_i \sim 10^3$, then $\epsilon \sim 10^{-3}$.

The expression of the steady-state solution of system is found by introducing the lumped species $NO_x = NO + NO_2$ and $O_x = O_3 + NO_2$ (References, sportisse 2000) in order to re-write equations (14)-(16) as:

$$\frac{\partial NO_x}{\partial t} + u \frac{\partial NO_x}{\partial x} = 0, \quad (17)$$

$$\frac{\partial O_x}{\partial t} + u \frac{\partial O_x}{\partial x} = 0, \quad (18)$$

$$\frac{\partial O_3}{\partial t} + u \frac{\partial O_3}{\partial x} = -\frac{\chi}{\epsilon}. \quad (19)$$

In this new form, and denoting $D/Dt = \partial/\partial t + u \partial/\partial x$, it can be seen that the lumped species NO_x and O_x are conserved in time, since

$$\frac{D NO_x}{Dt} = 0 \quad \text{and} \quad \frac{D O_x}{Dt} = 0.$$

As a consequence, for regions where the three species are initially present, the exact asymptotic value of the concentration of all species, NO^\dagger , NO_2^\dagger , and O_3^\dagger , can be found explicitly as a function of the initial concentration of the lumped species. This is achieved in two steps. First, by expressing the values of the steady state concentrations, NO^\dagger and NO_2^\dagger , as a function of the conserved lumped species as:

$$NO_x(0) = NO^\dagger + NO_2^\dagger \quad \text{and} \quad O_x(0) = O_3^\dagger + NO_2^\dagger, \quad (20)$$

and substituting them in equation (19). The system reaches a chemical steady state when $\chi = (NO) O_3 - 2 NO_2 = 0$, or equivalently when

$$[NO_x(0) - [O_x(0) - O_3^\dagger]]O_3^\dagger - 2[O_x(0) - O_3^\dagger] = 0, \quad (21)$$

which is a second order equation for the steady state of O_3^\dagger with solutions given by

$$O_3^\dagger = -\frac{1}{2} (2 + NO_x(0) - O_x(0)) \pm \frac{1}{2} \sqrt{(2 + NO_x(0) - O_x(0))^2 + 8O_x(0)} \quad (22)$$

And second, the values of NO^\dagger , and NO_2^\dagger can be found by substituting the (physically relevant) positive solution of (22) in equations (20). For time scales τ such that $\tau \gg 1/k$ (for $k = \min(k_1, k_2)$), the system will have reached chemical steady-state and from then on, equations (17)-(19) (and thus the original system (11)-(13)) will behave as a transport-only process propagating the steady-state concentrations with a constant velocity u .

3.2. Numerical experiments

We chose to solve equations (11)-(13) to simulate the fate of an instantaneous release containing the three chemicals over a 360 km one-dimensional region. The constant flow velocity was chosen to resemble realistic atmospheric values of $u = 10$ m/s. We prescribed a computational spatial domain, $x \in [0, L]$ for $L = 3000$ km, so that the plume would stay within the domain for the whole simulation time, $t \in [0, T]$ for $T = 10$ hours, and in order to not introduce any errors due to boundary conditions in the numerical advection operator. The values of $k_1 = 1000$ and $k_2 = 2000$ were chosen for the stiff chemistry operator. The effective stiffness of the chemistry with respect to the transport is $O(10^{-2})$ since $u \sim O(10)$. The initial conditions are given by $NO(x, 0) = NO_2(x, 0) = O_3(x, 0) = p(x)$, where

$$p(x) = \begin{cases} 1 & \text{if } x \in [720, 1080] \\ 0 & \text{elsewhere.} \end{cases}$$

In a 10-hour simulation time period, the initial release is advected exactly 360 km to the right, and the concentrations of all species have reached chemical equilibrium. According to expression (22), $O_3^\dagger = NO^\dagger = 1.236$, and $NO_2^\dagger = 0.764$. The exact solution at time $t = T = 10$ hours is explicitly given by $O_3(x, T) = NO(x, T) = 1.236 \times p(x - 360)$ and $NO_2(x, T) = 0.764 \times p(x - 360)$. This is our reference solution.

For the numerical simulations, we implemented an explicit, second order accurate (in space), one-dimensional advection-scheme based on the Lax-Wendroff method with superbee slope limiters (See Leveque, pp 112 for details), and used for the chemistry, the built-in implicit stiff-ODE integrator ode23 from Matlab. In order to minimize contributions to the numerical error, to the first term in inequality (2), from both the advection scheme and chemistry integrator, we utilized a very small internal advection time step, $\Delta t_\tau = 90$ seconds, and set the convergence relative-tolerance parameter to 10^{-3} in the routine ode23 (it adaptively chooses a small internal time step

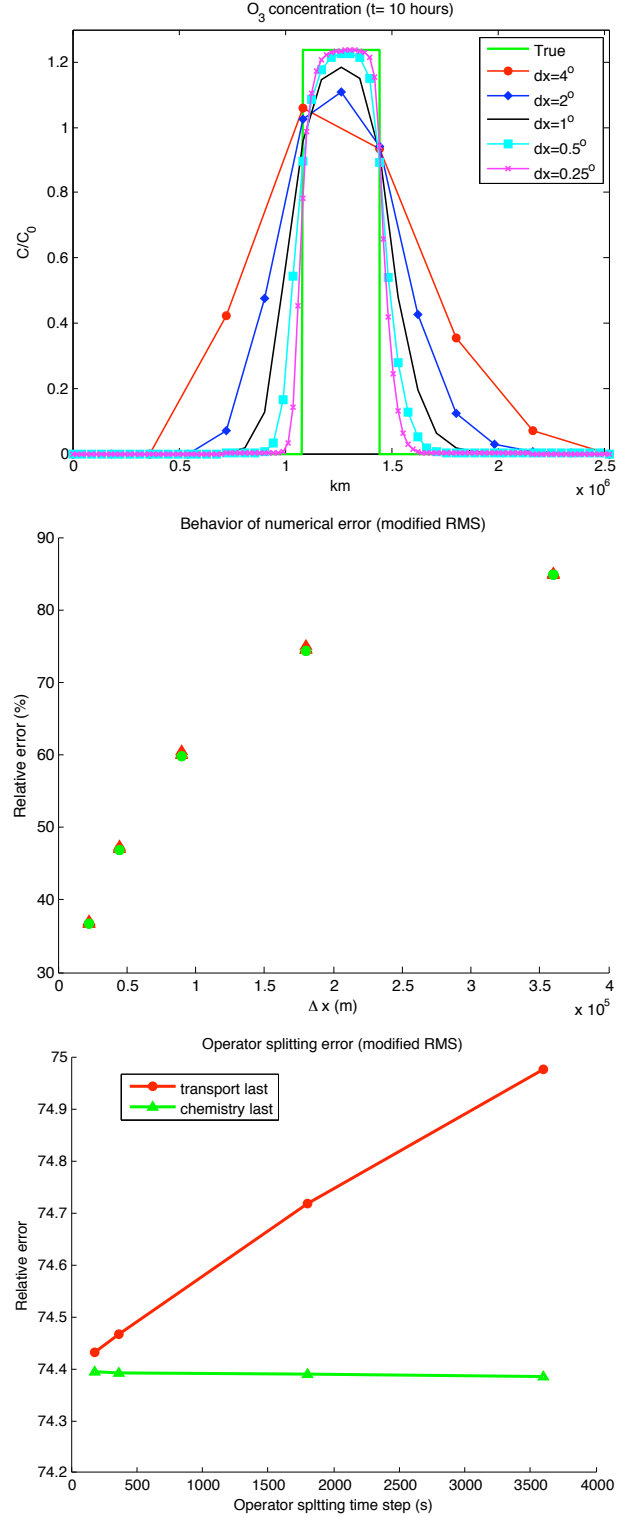


Figure 1: Behavior of numerical error in the one-dimensional transport-chemistry system. The top panel shows the analytical "true" and numerical solutions at different grid sizes of the system after a 10-hour simulation time. The middle panel shows the errors relative to the true solution with different grid sizes and operator splitting approaches. The bottom panel shows the behavior of the relative errors (RRMS) from the two operator splitting approaches, for fixed $\Delta x = 180$ km and different time steps, when compared to the analytic solution.

in order to meet the prescribed 0.1% error convergence criterion).

We solved equations (11)-(13) using multiple first order Godunov operator splitting approaches (where transport and chemistry were evaluated in different orders) for multiple operator-splitting time-steps, $\Delta t = 180, 360, 1800$ and 3600 seconds, and for multiple grid sizes $\Delta x = 22.5, 45, 90, 180$ and 360 km (the three largest grid sizes were chosen to resemble spatial resolutions of $4^\circ \times 5^\circ$, $2^\circ \times 2.5^\circ$, and $1^\circ \times 1.25^\circ$, in current 3D global CTMs). The results of these numerical simulations and the exact solution are plotted in the top plot of Figure 1. The numerical solutions corresponding to the multiple operator splitting approaches, for a given value of Δx , appear as a single curve since their differences were smaller than the line-width chosen for the plot.

The quantification of numerical errors was performed using the modified relative root mean square (RRMS), commonly used in 3D atmospheric chemistry simulations given by

$$d_{AB}(C_i) = \sqrt{\frac{1}{M} \sum_{\Omega} \left| \frac{C_i^A - C_i^B}{C_i^A} \right|^2} \quad (23)$$

where C_i^A and C_i^B are the concentrations of species i calculated in simulations A and B , respectively, Ω is the set of grid-boxes where C_i^A exceeds a threshold a , and M is the number of such grid-boxes. We used $a = 10^{-4}$, thus neglecting concentrations smaller than $\sim 0.01\%$ with respect to the original concentration. In our one-dimensional experiments, simulation A is the exact solution, and simulation B was one of the multiple Godunov operator splitting approaches. The second plot of Figure 1 shows the quantity $d_{AB} = (1/i) \sum_i d_{AB}(C_i)$ for $i = 3$ species, for the multiple values of Δt and Δx . In this plot, the red triangles represent simulations where transport was evaluated last, ($\chi - T$), and the green dots where chemistry was evaluated last ($T - \chi$). This plot confirms what is observed in the top plot, *i.e.*, the fact that the differences across the multiple operator splitting approaches, for a given Δx , are very small ($\leq 1\%$).

In the bottom plot of Figure 1, we further show the values of the numerical error for the two sequences, $\chi - T$ and $T - \chi$, for $\Delta x = 180$ km, for the multiple values of the operator splitting time-steps. We found this plot to be representative of the behaviour of the

numerical error for other values of Δx . Note that while the differences across the multiple approaches are very small, the interesting mathematical behaviour of the numerical error, discussed in section 2.1, can be observed. Indeed, the numerical error of the sequences $T - \chi$, where the chemistry (the stiff process) is evaluated last, produce better numerical results than their counter parts $\chi - T$. Moreover, $T - \chi$ sequences appear to be almost insensitive to the magnitude of the operator splitting time-step (the error even seems to grow as $\Delta t \rightarrow 0$ as reported in Sportisse, 2000) making them a preferred choice, since larger operator splitting time steps allow faster computations when exploiting the intrinsic parallelizable nature of the chemistry operator. The quality of results produced by sequences where transport is evaluated last, follows the traditional behaviour of linear analysis where the numerical error decreases as the operator splitting time decreases. Since the magnitude of these first order operator splitting errors was so small, we chose to not implement higher order operator splitting approaches.

While the bottom plot of Figure 1 shows a clear picture of the magnitude of operator splitting errors ($\leq 1\%$), we performed transport-only simulations in order to verify the magnitude of the numerical errors coming from the numerical advection scheme itself. The results of these simulations are shown in the top plot of Figure 2. Note that while the magnitude of the concentration of O_3 in these simulations is exactly one (since no chemistry is present), the numerically simulated profiles, for the different values of Δx , look very similar to those in the top plot of Figure 1. Indeed, when computing the modified RRMS error associated to these simulations, as shown in the bottom plot of Figure 2, the behaviour of the relative errors resembles the one observed in the middle plot of Figure 1. In short, the numerical errors coming from the choice of operator splitting are eclipsed by the largest component of the numerical error coming from the spatial discretization (second term in inequality (2)) in the numerical advection scheme.

Having chosen an initial condition in the shape of a step function in our experiments, caused our second order numerical advection scheme to behave as a first order scheme. Indeed the numerical error decreases close to linearly in our numerical experiments when using the L^2 -norm instead of the modified RRMS (plot not shown). Estimates for the numerical errors, in the form of an effective numerical diffusion, D_h , for 1D first order numerical advection schemes place their value at

$D_h \sim u\Delta x$, where u is the mean flow velocity and Δx the grid spacing. In our 1D experiments, these numerical diffusion is of the order $D \sim 10^6 \text{ m}^2/\text{s}$. Numerical diffusion in 3D global models (Lin and Rood (1996); Santillana (2013); Rastigeyev et al. (2007); Wild and Prather (2006); Pisso et al. (2009)) is estimated to be around $10^5 - 10^6 \text{ m}^2/\text{s}$. These 3D estimates place our one-dimensional experiments within a relevant range.

4. Numerical experiments using GEOS-Chem

Determining the exact magnitude of numerical errors in 3D global CTM simulations in the exact same way we did for our 1D prototype is not possible. This is due to the lack of an analytic expression for the solution to equations (1) in realistic circumstances (time-dependent winds, time-dependent chemistry rates changing throughout the geographic domain due to photolysis, time-dependent emissions). In order to estimate operator splitting errors in 3D CTMs, we can only compare the output of simulations where everything is kept the same except for the operator splitting sequence and the operator splitting time step. This is the strategy we present in this section, which in combination with the results from our one-dimensional simulations, allowed us to determine upper bounds of operator splitting errors in GEOS-Chem.

GEOS-Chem is a state-of-the-art 3D global model of tropospheric chemistry driven by assimilated meteorological observations from the Goddard Earth Observing System (GEOS) of the NASA Global Modeling and Assimilation Office (GMAO). The model simulates global tropospheric ozone-NO_x-VOC-aerosol chemistry. The full chemical mechanism for the troposphere involves over a hundred species and over three hundred reactions. The chemical mass balance equations are integrated using a Gear-type solver (Jacobson, 1995). Stratospheric chemistry is not explicitly simulated and it instead uses the Synoz cross-tropopause ozone flux boundary condition of McLinden et al. (2000). The model uses the flux form semi-Lagrangian advection scheme of Lin and Rood (1996). We used the GEOS-Chem model (v8-02-03) driven by the GEOS-5 data at the 4×5 horizontal resolution and 47 levels in the vertical. Detailed descriptions of the model are given by (Bey et al., 2001) and (Zhang et al., 2011). In this study, we initiate the model simulations on January 1, 2005 with model fields from a 6-month spin-up run, and focus on the weekly averaged model results for January 1-7, 2005.

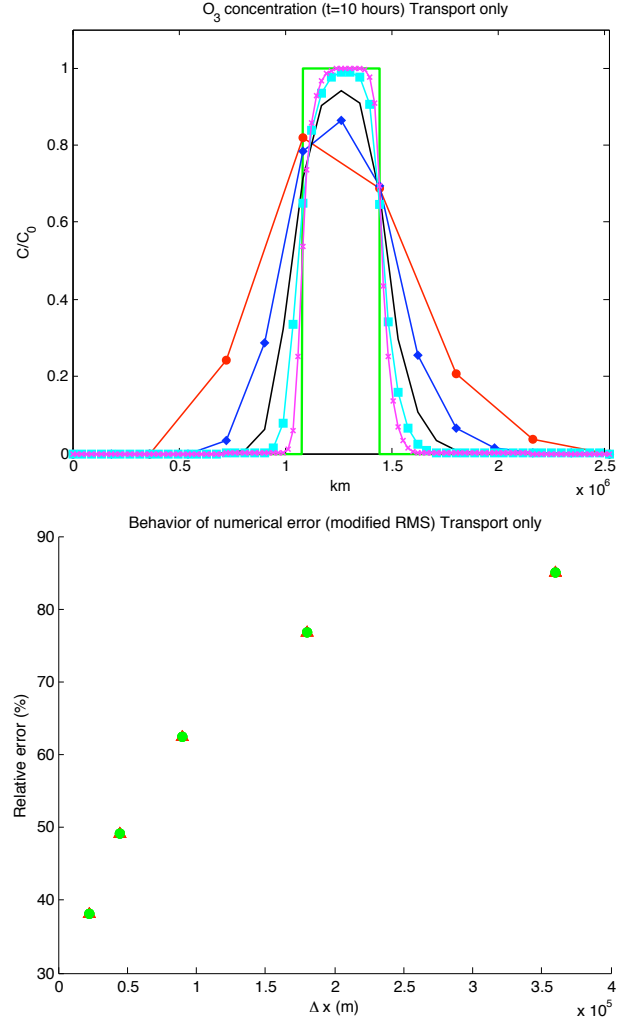


Figure 2: Behavior of numerical error in the one-dimensional transport-only system. The top panel shows the analytical “true” and numerical solutions at different grid sizes of the system after a 10-hour simulation time. The bottom panel shows the errors relative to the true solution with different grid sizes and operator splitting approaches.

Our strategy consisted of comparing the instantaneous concentration of several chemical species, after multiple one-week long, $4^\circ \times 5^\circ$ horizontal resolution, GEOS-Chem simulations (version v8-02-02), using two versions of the (default) second order Strang operator splitting method given by the sequences:

$$T(\Delta t/2)\chi(\Delta t)T(\Delta t/2) \quad \text{and} \quad \chi(\Delta t/2)T(\Delta t)\chi(\Delta t/2)$$

for different values of the operator-splitting time step Δt . These sequences are denoted as $T\chi T$ and $\chi T\chi$ respectively in the subsequent paragraphs. We used $\Delta t = 60, 30, 10, 2$ mins. In all these simulations, transport and chemistry were the only active mechanisms, all other mechanisms were turned off. The inactive mechanisms include: convective transport, planetary boundary layer mixing, and deposition. Emissions are treated as production rates distributed in the boundary layer and solved together in the chemistry operator.

We used the modified RRMS (23) with a threshold $a = 10^6$ molecules cm^{-3} to quantify the numerical differences in our global simulations. Figure 4 shows the relative differences between the reference simulation $\chi T\chi$ with $\Delta t = 2$ mins, and the other operator splitting approaches for multiple Δt 's. Note that the maximum differences across simulations (and species) are of the order of $\sim 10\%$.

We also plotted the differences between multiple operator splitting strategies from our one-dimensional prototype results for $\Delta x = 180$ km, using the sequence $T - \chi$ for $\Delta t = 3600$ sec as a reference in Figure 3. Note that while the bottom plot of Figure 1 shows that operator splitting (relative) errors are less than 1% (when comparing to the analytic solution), the relative differences between simulations using alternative operator splitting methods may be as large as 10%. This is roughly the same magnitude of the differences observed between the 3D simulations shown in Figure 4.

Note that we chose the sequence $\chi T\chi$ with $\Delta t = 2$ mins as the reference simulation for our 3D experiments, instead of the sequence $\chi T\chi$ with $\Delta t = 60$ that would have been suggested by our 1D experiments (as in Figure 3). The reason for this is shown in Figure 5, where we can see that the differences between simulations with different operator splitting sequences but with the same time step, get smaller as Δt gets smaller. This behaviour would be expected from a converging operator splitting method where none of the

operators is stiff and where the order of evaluation of the operators is not relevant. An alternative explanation could be that the operator splitting errors are very small and what we are observing is the convergence of the time-integration of each operator, separately, as Δt gets small. This would suggest that the numerical errors of the time-integration of the transport and the chemistry contribute significantly to the first term (involving Δt) on the right hand-side of inequality (2), and should be comparable, in magnitude, to those observed between different operator splitting sequences.

In order to investigate this, we plotted the differences between simulations where the only active mechanism was either chemistry or transport, for multiple Δt 's, while keeping all other parameters exactly the same as in the previous simulations. The results are plotted in Figure 6 for the chemistry-only simulations, and in Figure 7 for the transport-only simulations. These two plots show that indeed the numerical errors arising from the time-integration of each of the operators separately lead to differences of the same magnitude as those observed in the operator splitting simulations. We also observe that the differences get smaller as Δt decreases suggesting numerical convergence. This comparable differences make it hard to disentangle a sharp estimate of the operator splitting in 3D.

Note also that in our one dimensional prototype a cleaner analysis was achieved since we chose a smaller internal time step ($\Delta t_\tau = 90$ seconds) to integrate the (explicit-in-time) transport operator than the operator splitting time step ($180 \text{ seconds} \leq \Delta t \leq 60 \text{ mins}$). This choice reduced the contribution to the numerical errors involving Δt in inequality (2) from the transport integration. In order to save computational time in GEOS-Chem (and in most CTMs), however, the time step of the (explicit-in-time) transport scheme is chosen to be equal to the operator splitting time step leading to larger numerical errors.

In our one dimensional prototype, the chemistry operator was solved using an adaptive time-integration routine with very tight convergence constraints, thus reducing numerical errors. The time-integration of the chemistry operator in GEOS-Chem uses an adaptive time stepping strategy (Jacobson (1995)) that chooses the magnitude of the time step in order to meet (absolute and relative) convergence requirements set by the user. These parameters are not very tight in GEOS-Chem in the interest of computational performance and lead to the differences between simulations shown in Figure 6.

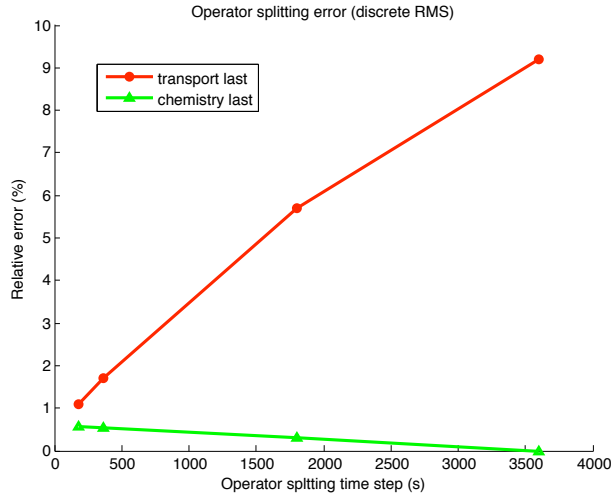


Figure 3: Behavior of the relative errors (RRMS) from the two operator splitting approaches, for fixed $\Delta x = 180\text{km}$ and different time steps, when compared to the reference solution obtained with the sequence $T - \chi$ for $\Delta t = 3600$ seconds.

Despite all of these numerical issues, we highlight the fact that we can establish an upper limit of about a 10% for the magnitude of operator splitting errors based on the results of our multiple simulations in 3D. Moreover, we show that differences of the single chemical species with largest discrepancies across simulations, Isoprene, are not significant in Figures 9, 8, and 10, for chemistry only simulations, transport only simulations, and different sequences of operator splitting methods, respectively. From these plots and the results of our one-dimensional prototype, we hypothesize that the operator splitting errors may be much smaller than 10%.

We also highlight the fact that we did not pursue further efforts to show that the sequences evaluating the chemistry at the end of the time step in 3D are more accurate, since our one-dimensional prototype, as well as multiple studies in global CTMs (Rastigeyev et al., 2007; Prather et al., 2008; Santillana, 2013), suggest that the numerical errors associated to the transport integration, at current spatial resolutions, are significantly larger than those observed in operator splitting methods. In our one-dimensional prototype, subsequent reductions in the spatial resolution lead to significant improvements in the accuracy of the numerical solution globally (for any operator splitting sequence). Whereas a better choice of operator splitting (where chemistry is evaluated last) leads to a very modest improvement at a given spatial resolution Δx .

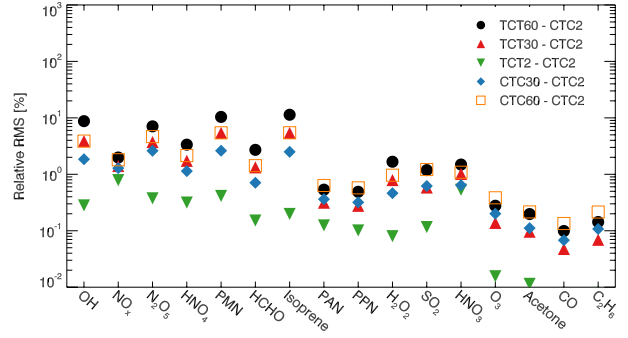


Figure 4: Behavior of numerical error in the GEOS-Chem 3-D model simulations. Here TCT denotes Transport-Chemistry-Transport, CTC denotes Chemistry-Transport-Chemistry, and the numbers denotes operator splitting time steps in minutes. Relative RMS relative to the CTC2 model simulation are shown for different chemical species with lifetimes ranging from seconds (OH) to months (CO , C_2H_6).

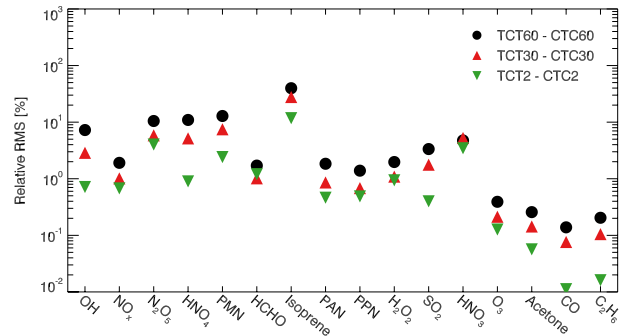


Figure 5: Behavior of numerical error in the GEOS-Chem 3-D model simulations. Here TCT denotes Transport-Chemistry-Transport, CTC denotes Chemistry-Transport-Chemistry, and the numbers denotes operator splitting time steps in minutes. Relative RMS for different operator splitting approaches for fixed time steps: $\Delta t = 2, 30, 60$ mins.

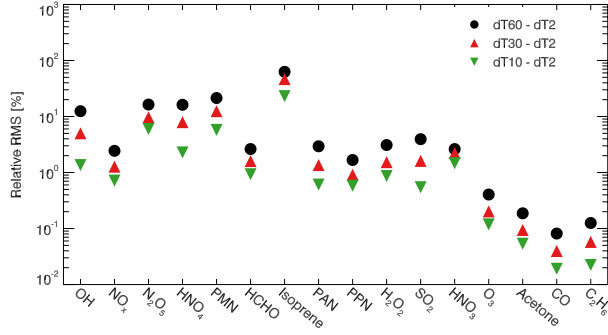


Figure 6: Behavior of numerical error in the GEOS-Chem 3-D model simulations. Relative RMS for chemistry-only simulations using different time steps: $\Delta t = 2, 30, 60$ mins.

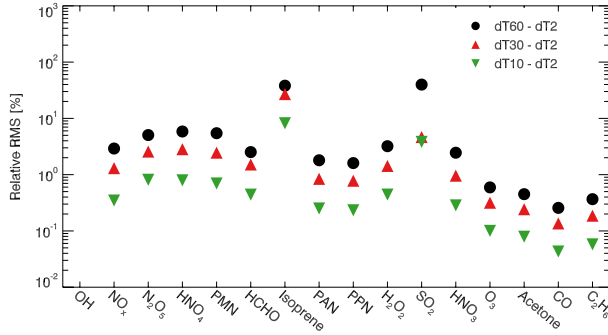


Figure 7: Behavior of numerical error in the GEOS-Chem 3-D model simulations. Relative RMS for transport-only simulations using different time steps: $\Delta t = 2, 30, 60$ mins.

5. Conclusions

We have presented a way to characterize operator splitting errors in the context of atmospheric chemistry modeling. Our approach numerically extends one-dimensional linear results to non-linear 1D and 3D cases. These numerical findings are relevant to global atmospheric chemistry modeling. Our findings suggest that stiff operators should be evaluated lastly in operator splitting methodologies. This is consistent with linear results. Differences of approximately 10% across species are found when comparing the outputs of global simulations using different operator splitting approaches, using multiple splitting time steps. This, in combination with our one-dimensional results, suggests that operator splitting errors do not exceed 10% relative errors in global simulations. We show also, that in current spatial resolutions, the numerical diffusion errors introduced in global atmospheric chemistry models eclipse errors emerging from operator splitting techniques.

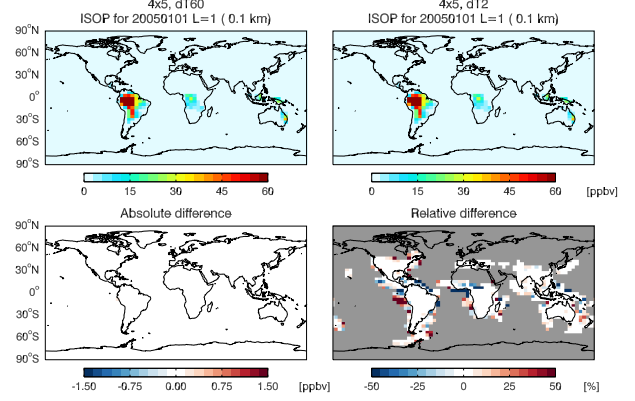


Figure 8: Comparison of isoprene concentrations using different time steps for GEOS-Chem transport-only simulations. Isoprene concentrations at the surface level from the model simulation with time step of 60 minutes (top-left panel) are compared to the model simulation with time step of 2 minutes (top-right panel). Absolute (bottom-left) and relative differences (bottom-right) are also shown.

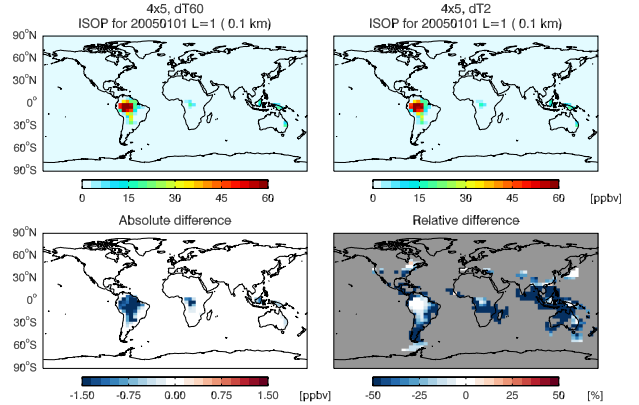


Figure 9: Comparison of isoprene concentrations using different time steps for GEOS-Chem chemistry-only simulations. Isoprene concentrations at the surface level from the model simulation with time step of 60 minutes (top-left panel) are compared to the model simulation with time step of 2 minutes (top-right panel). Absolute (bottom-left) and relative differences (bottom-right) are also shown.

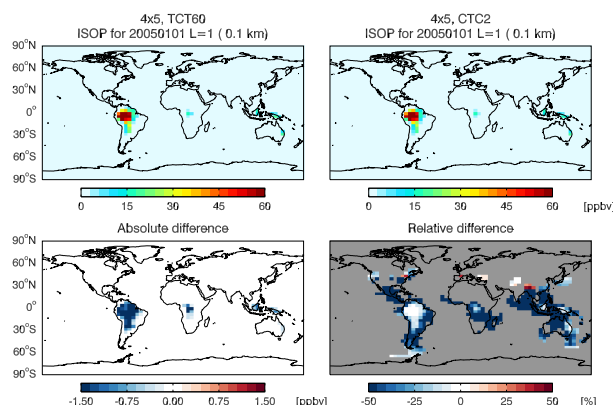


Figure 10: Comparison of isoprene concentrations using Transport-Chemistry-Transport (time step of 60 minutes) versus Chemistry-Transport-Chemistry (time step of 2 minutes).

Acknowledgements

MS and LZ would like to thank the technical assistance provided by Claire Carouge. MS would like to thank Jonathan Pines for his involvement in the exploratory phases of this project.

References

- Bey I., D. J. Jacob, R. M. Yantosca, J. A. Logan, B. Field, A. M. Fiore, Q. Li, H. Liu, L. J. Mickley, and M. Schultz. Global modeling of tropospheric chemistry with assimilated meteorology: Model description and evaluation, *Journal of Geophysical Research*, 106, 23,073-23,096, 2001.
- Brenner, S. C., and Scott R. The mathematical theory of finite element methods. Vol. 15. Springer Science and Business Media, 2008.
- Enting, I. G. Inverse Problems in Atmospheric Constituent Transport. Cambridge University Press. 2002.
- Ern, A., and Guermond, J.L. Theory and practice of finite elements, vol. 159 of Applied Mathematical Sciences. 2004.
- Hundsdoerfer W. and Verwer J.G.: Numerical Solution of Time-Dependent Advection-Diffusion-Reaction Equations, Springer Series in Computational Mathematics, 33, Springer. 2003.
- A. Iserles.: A first course in the numerical analysis of differential equations, Cambridge University Press, 44, 2009.
- Jacobson M. Z.: Computation of Global Photochemistry with SMVGEAR-II, *Atmospheric Environment*, 29(18), 2541-2546, 1995.
- Lanser D., Verwer J.G.: Analysis of operator splitting for advection-diffusion-reaction problems from air pollution modelling, *Journal of Computational and Applied Mathematics*. 111, 201216
- Lin, S.J. and R. B. Rood. Multidimensional flux-form semi-Lagrangian transport schemes. *Monthly Weather Review* 124.9, 1996.
- Lowe, R. and Tomlin, A.: Low-dimensional manifolds and reduced chemical models for tropospheric chemistry simulations, *Atmospheric Environment*, 34, 2425-2436, 2000.
- McLinden, C. A. et al. Stratospheric ozone in 3-D models: A simple chemistry and the cross-tropopause flux, *J. Geophys. Res.*, 105(D11), 1465314666, 2000.

- Pisso, I., et al. Estimation of mixing in the troposphere from Lagrangian trace gas reconstructions during long-range pollution plume transport. *Journal of Geophysical Research: Atmospheres*, 114.D19, 2009.
- Prather, M. J., et al. Quantifying errors in trace species transport modeling. *Proceedings of the National Academy of Sciences* 105.50, 2008
- Rastigejev, Y., M. P. Brenner, and D. J. Jacob. Spatial reduction algorithm for atmospheric chemical transport models. *Proceedings of the National Academy of Sciences* 104.35, pp 13875-13880, 2007.
- M. Santillana, P. Le Sager, D. J. Jacob, and M. P. Brenner.: An adaptive reduction algorithm for efficient chemical calculations in global atmospheric chemistry models, *Atmospheric Environment*, Volume 44, Issue 35, pp 4426-4431, 2010.
- M. Santillana.: Quantifying the loss of information in source attribution problems using the adjoint method in global models of atmospheric chemical transport. *arXiv.org*: 1311.6315, 2013
- B. Sportisse: An Analysis of Operator Splitting Techniques in the Stiff Case, *Journal of Computational Physics*, 161, 140168, 2000.
- G. Strang: On the construction and comparison of difference schemes. *SIAM J. Numer. Anal.* 5, 3 September 1968, 506517.
- Wild, O., and M. J. Prather. Global tropospheric ozone modeling: Quantifying errors due to grid resolution. *Journal of Geophysical Research: Atmospheres* 111.D11 (2006).
- H. Zhang, J. C. Linford, A. Sandu, and R. Sander. Chemical Mechanism Solvers in Air Quality Models, *Atmosphere* 2011, 2, 510-532.
- Zhang, L. et al. Improved estimate of the policy-relevant background ozone in the United States using the GEOS-Chem global model with 1/2 2/3 horizontal resolution over North America, *Atmos. Environ.*, 45, 67696776, 2011.